

## Microcompression of nanocrystalline nickel

B. E. Schuster

Department of Mechanical Engineering, Johns Hopkins University, Baltimore, Maryland 21218  
and Weapons and Materials Research Directorate, Army Research Laboratory, Aberdeen Proving Ground, Maryland 21005

Q. Wei,<sup>a)</sup> H. Zhang, and K. T. Ramesh<sup>b)</sup>

Department of Mechanical Engineering, Johns Hopkins University, Baltimore, Maryland 21218

(Received 31 August 2005; accepted 14 February 2006; published online 8 March 2006)

Microcompression is a technique that was developed as a means to probe the properties of micrometer-sized specimens using a modification of a conventional nanoindentation system. We use this technique to present the first uniaxial compressive data on electrodeposited nanocrystalline nickel (a material system where the grain size is much smaller than the specimen size). The compression-tension asymmetry of this nanocrystalline material is also discussed. © 2006 American Institute of Physics. [DOI: 10.1063/1.2183814]

The mechanical properties and deformation behavior of face-centered-cubic nanocrystalline nickel (nano-Ni) have been closely examined in recent years. The deformation behavior has been examined in molecular dynamics simulations,<sup>1</sup> in tension,<sup>2-4</sup> and in conventional nanoindentation.<sup>4,5</sup> Often, the experimental studies focus on commercially available electrodeposited nano-Ni in thin film or foil geometries where the sample thickness is typically on the order of hundreds of microns. This arrangement lends itself well to tension and to nanoindentation, but not to conventional compression experiments. Advances in micromachining techniques [e.g., focused ion beam (FIB)] allow for the fabrication of micrometer sized compression specimens (microposts). Recent innovations by Uchic *et al.*<sup>6-9</sup> provide a means to probe the compressive behavior of these microposts. In this letter, we bring together these advances to present, for the first time, the compressive properties of electrodeposited nanocrystalline nickel.

Microcompression was first introduced by Uchic *et al.*<sup>6,7,9</sup> as a means to examine size effects in micrometer-sized single crystal compression specimens using a truncated Berkovich tip in a conventional nanoindenter. In past efforts, FIB micromachining has been the primary method of producing compression specimens using currents of Ga ions as high as several thousand pA.<sup>6-9</sup> These previous studies have examined size scale effects on single crystal plasticity. Our work, in contrast, focuses on the compressive properties of a material system in which the grain size is three orders of magnitude smaller than the specimen size.

We use a new two-step fabrication process to produce the micrometer-sized compression specimens with minimal (or no) use of expensive FIB micromachining. The process involves use of microelectrodischarge machining ( $\mu$ EDM) combined with polycrystalline diamond grinding (PCD) and allows for the production of multiple compression specimens that are well aligned, have relatively uniform dimensions (little taper) and a small postfillet radius. These are important

characteristics for such microcompression experiments as demonstrated in the recent analysis by Zhang *et al.*<sup>10</sup>

$\mu$ EDM was originally developed to drill micrometer sized holes in inkjet nozzles. This noncontact form of machining relies on pulsating electrical discharge between the work piece and an electrode for material removal. Further improvements have included the adaptation of a three-axis stage to allow for three-dimensional milling. In this study, a 100  $\mu$ m diameter electrode was used in a Panasonic Micro-EDM (MG-ED72W) with a three-axis stage to create arrays of 20 nanocrystalline nickel pillars. A damage zone  $\sim$ 1  $\mu$ m thick is left on the surface of the nanocrystalline microposts after the  $\mu$ EDM process.<sup>9</sup> To remove the  $\mu$ EDM damage layer and to improve the geometry to the guidelines set by Zhang,<sup>10</sup> PCD grinding is employed. A  $\mu$ EDM is first used to machine a PCD right-cylindrical tool. The PCD tool is then placed in a V-bearing arrangement where it is rotated at 3000 rpm by a dc motor and scanned across the array of nano-Ni pillars which, again, are set on a three-axis machining platform. The nominal dimensions of the finished posts are 20  $\mu$ m on a side with a square cross section and 2:1 aspect ratio. The resulting 4  $\times$  5 array of posts is shown in Fig. 1(a) with an expanded view of a typical pillar shown in Fig. 1(b). The pillar dimensions are individually examined in a JEOL 6460 scanning electron microscope.

Commercially available nanocrystalline nickel was the focus of this study. Electrodeposited foils that are 150  $\mu$ m in thickness were provided by Integran Technologies Inc. The nano-Ni in this study comes from the as received state from the same batch examined by Wang.<sup>2,3</sup> The actual mean grain size was found to be 29 nm. More details on this batch of material including x-ray diffraction data, transmission electron microscopy micrographs, and impurity contents are provided by Wang.<sup>2,3</sup>

The nanocrystalline Ni pillars were studied in microcompression using the process described in detail by Uchic.<sup>9</sup> Since there are about a million grains across the cross section and about a billion grains in each post, we are able to obtain the effective response of the bulk material with this technique. An MTS Nanoindenter XP with the continuous stiffness measurement (CSM) extension was used with a truncated Berkovich indenter to apply the compressive load. The load and displacement along with corresponding stiffness

<sup>a)</sup>Present address: Department of Mechanical Engineering and Engineering Science, University of North Carolina at Charlotte, 9201 University City Boulevard, Charlotte, NC 28223.

<sup>b)</sup>Author to whom correspondence should be addressed; electronic mail: ramesh@jhu.edu

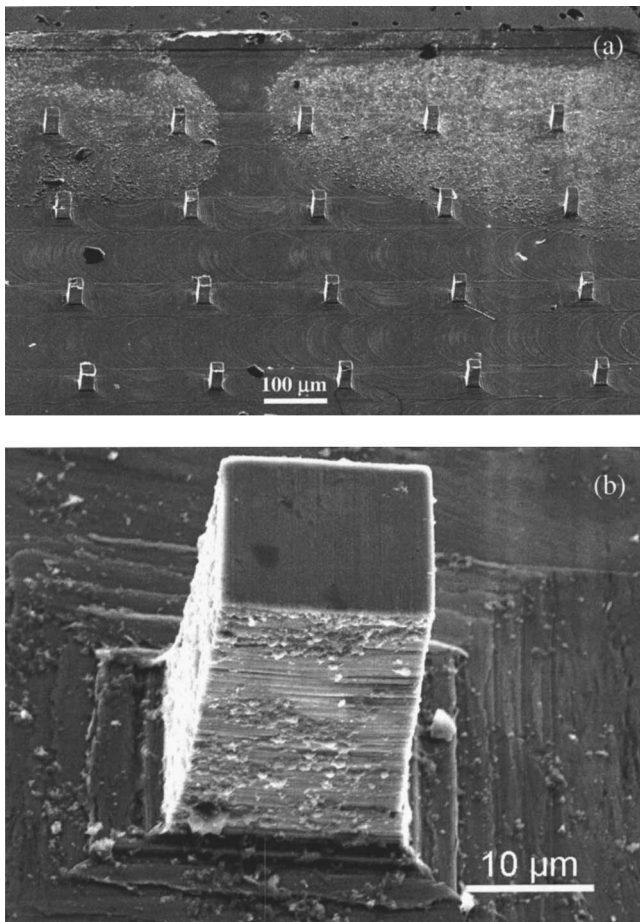


FIG. 1. (a) Array of nanocrystalline Ni posts from  $\mu$ EDM followed by PCD grinding. (b) Enlarged view of (a) with a typical post nominally  $20\ \mu\text{m}$  on a side with a 2:1 aspect ratio.

were recorded for these specimens deformed at a strain rate of  $10^{-3}\ \text{s}^{-1}$ . Following the method proposed by Zhang *et al.*,<sup>10</sup> the pillar compliance was corrected for the effect of the elastic base. The base contact area, including fillet radius, was related to a cylindrical area with an equivalent contact radius  $r_c$ . The base compliance  $C_b$  of the microposts was found from<sup>10</sup>

$$C_b = \frac{1 - \nu^2}{2E\eta r_c},$$

where  $E$  is the elastic modulus for Ni,  $\nu$  is Poisson's ratio, and  $\eta=1.42$ . This base compliance was subtracted from the measured compliance and the corresponding stress and strain measures were corrected accordingly.

The resulting stress-strain curves are plotted in Fig. 2. The nano-Ni specimens showed very consistent compressive behavior. The compressive yield strength at 2% offset was an average of  $1210 \pm 20\ \text{MPa}$ . The maximum strength was repeatable for each case and was  $1498 \pm 10\ \text{MPa}$  as seen in Fig. 2. The measured elastic modulus for unloading is  $95\ \text{GPa}$ ; small in comparison to theoretical predictions. Zhang *et al.*<sup>10</sup> showed that alignment has a profound effect on the measured elastic modulus, yet this effect on the apparent elastic modulus comes without detriment to strength measurement. In other experiments not presented here, we do not observe material failure in deformations up to 25% (an example of such a typical deformed micropost is shown in Fig. 3). However, we sometimes see evidence of structural (as opposed to ma-

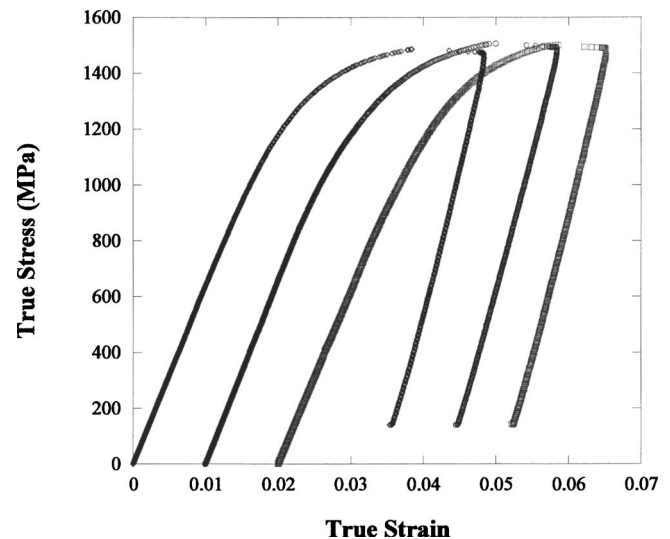


FIG. 2. Repeatable compressive response of nanocrystalline nickel posts with consistent yield strengths and peak strengths.

terial) failure or buckling that may occur at strains less than 10%. Local material variations in each post might trigger such failures. Materials with low strain hardening, such as nano-Ni, are also prone to plastic buckling in microcompression (although the contact friction between the indenter tip and compression post has been shown to suppress plastic buckling).<sup>10</sup> The effects of imperfect contact and minute misalignment on the measured elastic modulus and critical strain for plastic buckling have not been investigated experimentally using microcompression.

This batch of material was also examined by Wang.<sup>2,3</sup> They report a flow strength (at 3.5% strain) of  $1260\ \text{MPa}$  in tension ( $\sigma_T$ ) and a microhardness ( $H$ ) of over  $5.5\ \text{GPa}$ .<sup>2,3</sup> Our microcompression results show a compressive flow strength ( $\sigma_C$ ) at 3.5% strain of  $1460\ \text{MPa}$ , 16% higher than Wang's tensile values, i.e., the compression-tension asymmetry is  $\sigma_C/\sigma_T=1.16$  (note that we compare the flow strengths at a given strain rather than yield due to general uncertainties in measuring initial yield). In contrast, one obtains  $\sigma_C/\sigma_T=1.5$  if the compressive strength ( $\sigma_C$ ) is estimated using the approximation that  $H \sim 3\sigma_C$  and using Wang's measured microhardness.

Lund and Schuh<sup>1</sup> addressed compression-tension asymmetry across a broad range of grain (ultra fine grained, nano-2, and nano-1) sizes using molecular dynamics (MD)

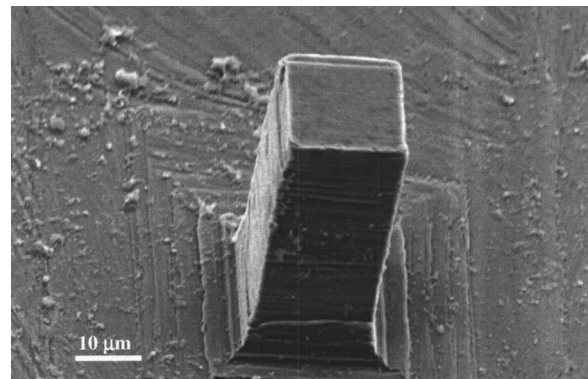


FIG. 3. Typical deformed nanocrystalline Ni micropost. Permanent plastic deformation is observed without structural failure.

simulations and analysis, comparing with Cheng *et al.*<sup>11</sup> who addressed compression-tension asymmetry using a strength model based on dislocation emission from grain boundary sources for the nano-2 and UFG regimes. The latter model relates the uniaxial strength of materials to the self-energy of a dislocation under pressure following the formulation of Jung *et al.*<sup>12</sup> Lund and Schuh<sup>1</sup> applied the elastic constants of Ni to the Cheng *et al.* model, and demonstrated a gradual increase in compression-tension asymmetry with decreasing grain size in the nano-2 and UFG regimes. Jiang and Weng<sup>13</sup> present analytical solutions for Cu using a weighted average of a crystalline phase (with grain size dependent mechanical properties) and an amorphous grain boundary (with size independent properties). In these analyses, the volume fraction of the grain boundaries increases with decreasing grain size and thereby affects the overall response. For example, the analysis applied to Cu shows increasing compression-tension asymmetry with decreasing grain size with a peak in or near to the nano-1 to nano-2 transition.

Our study closely matches the predictions by Jiang *et al.*<sup>13</sup> of the compression-tension asymmetry ( $\sim 1.2$ ) for Cu at a similar grain size. At a similar grain size, the CSM model<sup>11</sup> applied to Ni underestimates the measured asymmetry.<sup>1</sup> This suggests that, at this grain size, there are other contributing deformation mechanisms besides the emission of grain boundary dislocations, perhaps including normal stress or pressure dependent mechanisms. Can it be shown experimentally that there is a peak in the asymmetry as suggested by Jiang *et al.*?<sup>13</sup> Using microcompression, we have established a means to directly examine the asymmetry for this electrodeposited nanocrystalline nickel system without estimates of compressive strength based on hardness. This approach could be used to address the latter question, among several others of interest to the materials science community

relating to the relative stability of nanocrystalline materials under various stress states.

Microcompression experiments offer a means to not only examine the response of single crystal microposts, but also to experimentally examine the compressive response of a wide range of nanocrystalline metals. The ability to fabricate and test pillars as small as several hundred nanometers may also offer future opportunities for direct comparisons of experimental and MD results.

The authors would like to acknowledge Jerry Mraz and SmalTec International for providing the  $\mu$ EDM and PCD machining. This work is supported by the U.S. Army Research Laboratory through Grant No. DAAL01-96-2-0047 and ARMAC-RTP Cooperative Agreement No. DAAD19-01-2-0003. This work was performed under the auspices of the Center for Advanced Metallic and Ceramic Systems (CAMCS) at the Johns Hopkins University.

<sup>1</sup>A. C. Lund and C. A. Schuh, *Acta Mater.* **53**, 3193 (2005).

<sup>2</sup>Y. M. Wang, S. Cheng, Q. Wei, E. Ma, T. G. Nieh, and A. Hamza, *Scr. Mater.* **51**, 1023 (2004).

<sup>3</sup>Y. M. Wang and E. Ma, *Appl. Phys. Lett.* **85**, 2750 (2004).

<sup>4</sup>R. Schwaiger, B. Moser, M. Dao, N. Chollacoop, and S. Suresh, *Acta Mater.* **51**, 5159 (2003).

<sup>5</sup>R. A. Mirshams and P. Parakala, *Mater. Sci. Eng., A* **372**, 252 (2004).

<sup>6</sup>M. D. Uchic, D. M. Dimiduk, J. N. Florando, and W. D. Nix, *Mater. Res. Soc. Symp. Proc.* **753**, BB1.4 (2003).

<sup>7</sup>M. D. Uchic, D. M. Dimiduk, J. N. Florando, and W. D. Nix, *Science* **305**, 986 (2004).

<sup>8</sup>J. R. Greer, W. C. Oliver, and W. D. Nix, *Acta Mater.* **53**, 1821 (2005).

<sup>9</sup>M. D. Uchic and D. M. Dimiduk, *Mater. Sci. Eng., A* **400**, 268 (2005).

<sup>10</sup>H. Zhang, B. E. Schuster, Q. Wei, and K. T. Ramesh, *Scr. Mater.* **54**, 181 (2006).

<sup>11</sup>S. Cheng, J. A. Spencer, and W. W. Milligan, *Acta Mater.* **51**, 4505 (2003).

<sup>12</sup>J. Jung, *Philos. Mag. A* **43**, 1057 (1981).

<sup>13</sup>B. Jiang and G. J. Weng, *Metall. Mater. Trans. A* **34A**, 765 (2003).